

55, 1035 (1965).

<sup>16</sup>F. J. Comes and A. Elzer, *Z. Naturforsch. A* **23**, 133 (1968).<sup>17</sup>R. B. Cairns and J. A. R. Samson, *Phys. Rev.* **139**,

A1403 (1965).

<sup>18</sup>F. J. Comes, F. Speier, and A. Elzer, *Z. Naturforsch. A* **23**, 125 (1968).

PHYSICAL REVIEW A

VOLUME 7, NUMBER 3

MARCH 1973

## Energy Dependence of the Total Cross Section for He-He Collisions from 0.30 to 3.00 keV<sup>\*†</sup>

W. J. Savola, Jr., F. J. Eriksen, and E. Pollack

*Physics Department, University of Connecticut, Storrs, Connecticut 06268*

(Received 21 September 1972)

The total cross section for scattering of He by He is measured at 100-eV intervals in an energy range from 0.30 to 3.00 keV. Measurements are made using detector angular resolutions of 0.056° and 0.260°. The cross section is found to decrease monotonically from 12.5 to 5.0 Å<sup>2</sup> and from 7.0 to 2.6 Å<sup>2</sup>, respectively, as the energy increases. Small-angle differential measurements are also made out to scattering angles of 1.25° at incident energies of 1.80 and 3.00 keV. At 3.00 keV a He<sup>+</sup> signal is found at scattering angles beyond 0.8°. The ratio of the ion to the total signal increases to about 10% at 1.25°. The total-cross-section data are used to infer a potential.

### I. INTRODUCTION

Collisions between beams of fast neutral atoms and thermal target atoms are generally studied because they can provide useful information on short-range interactions which occur in the colliding system. Studies of such collisions have been successful in yielding values for interatomic potentials which could then serve as a check on approximations employed in theoretically calculating interatomic potentials. Experimental results have also provided data which are useful in predicting high-temperature kinetic properties of gases.

Although it is possible to investigate short-range interactions by making differential cross-section measurements, such measurements usually have been made for ion-atom systems with very little differential work having been done on atom-atom collisions. Experimental studies concerned with atom-atom collisions have generally involved measurements of the energy dependence of the total cross section for scattering a fast neutral beam beyond a detector of fixed acceptance angle. This is the technique employed in the present study. In pioneering investigations, Amdur and co-workers<sup>1,2</sup> have measured such total cross sections for numerous neutral systems (see Ref. 2 for a discussion of the neutral experiments and additional references to the literature). Similar measurements have recently been made by Kamnev, Belyaev, and Leonas.<sup>3-5</sup> In addition, several of the important problems relating to the interpretation of experimental data (including quantum-scattering corrections and inelastic-scattering effects)

have been discussed in a review article by Mason and Vanderslice.<sup>6</sup>

The present experiment measures the energy dependence of the total cross section for the He-He collision in a range from 0.30 to 3.00 keV (in 100-eV intervals) at two different detector angular resolutions. One of the detector angular resolutions selected is sufficiently high so that quantum-scattering effects may arise at the lower energies. In addition, differential measurements are made to ascertain the contribution of small-angle inelastic scattering to the measured total cross sections. All measurements are made with fast He beams formed from mass-analyzed He<sup>+</sup>. Hole-hole geometries rather than combinations of holes and slits are used for collimation of the incident and scattered beams.

### II. APPARATUS

Figure 1 shows a schematic diagram of the apparatus. The operation of the electron-impact-ion source (A), extractor (B), lenses (C), and magnet (D) has been previously described.<sup>7,8</sup> A neutral beam is produced in the charge-exchange region (E) by resonant charge-exchange of the mass-analyzed He<sup>+</sup> with He at a pressure of about 30 μ. The charge-exchange region is 0.8 in. in diameter, and holes at either end define a charge-exchange path about 1.2 in. long. Emerging from the hole at (F) is a composite beam of He<sup>+</sup> ions and He neutrals. An electric field between two plates (G) deflects the ions into a Faraday cup monitor (H), while the neutrals pass through a collimating hole (I) and form the incident beam. The holes at (F) and

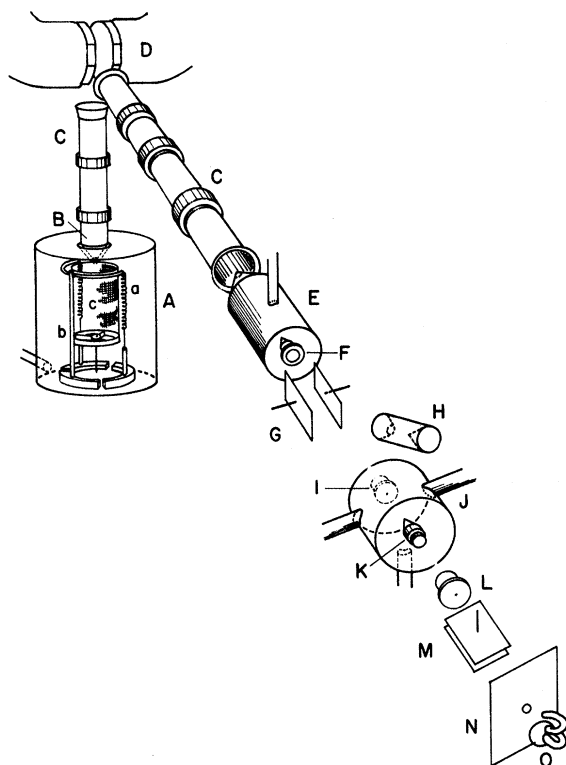


FIG. 1. Schematic of the apparatus.

(I) determine the incident collimation and are 0.0044 and 0.0022 in. in diameter, respectively; they are 4.18 in. apart, which results in a geometric angular resolution of  $0.045^\circ$ .

Collisions between the incident beam and the target gas occur primarily in the scattering chamber (J). The scattering length of 0.625 in. is determined by the distance between collimation buttons (I) and (K). One port leading into the scattering chamber connects to a capacitance manometer and also to a miniature ionization gauge (Bayer-Alpert type). Another port admits scattering gas into (J), and the third (bottom) connects the scattering chamber to a large-volume ballast tank.

The angular resolution of the detector is determined by small holes in two inserts located at (K) and (L); these two holes move with the detector chamber allowing differential scattering measurements to be made. The holes (K) and (L) are of diameters 0.0044 in. (0.0044 in.) and 0.0037 in. (0.033 in.), respectively, and a distance between them of 4.125 in. results in a geometric angular resolution of  $0.056^\circ$  ( $0.260^\circ$ ). The beam passes through a charge-state analyzer consisting of two gold-plated electrodes (M) and is detected by a channeltron multiplier (O); A plate (N) with a small hole in it defines the entrance to the multiplier.

Standard electronic equipment is used to count the resulting pulses.

### III. EXPERIMENTAL PROCEDURE

The general procedure involves the production of a fast He beam, attenuation of this beam by He scattering gas, and a measurement of the transmitted beam intensity as a function of scattering-gas pressure. The detected signal  $I$  is given by

$$I = I_0 e^{-n\sigma l}, \quad (1)$$

where  $I_0$  is the incident-beam intensity,  $n$  the scattering-gas density,  $l$  the effective path length,<sup>7</sup> and  $\sigma$  the cross section for scattering a beam atom beyond the detector acceptance angle.

Since the incident neutral beam is produced by charge exchange, the beam may include fast metastable atoms, which would cause difficulties in interpreting the experimental results. Although forward-scattered He metastables are kinematically allowed, the metastable state is probably excited by a curve-crossing mechanism.<sup>9</sup> This mode of excitation requires a relatively hard collision, and if small enough collimation holes are employed both before and after charge exchange, a negligible metastable population in the incident neutral beam can be ensured. Holes (F) and (I) in Fig. 1 are sufficiently small to block the metastable component generated by a narrow incident He<sup>+</sup> beam. To check divergence in our incident He<sup>+</sup> beam a high-angular-resolution precollimating system (consisting of two holes of diameters 0.0108 and 0.0088 in. separated by 1.117 in.) is placed between the last lens and the charge-exchange cell (E) for several cross-section measurements. To within the accuracy of our measurements there are no differences in the cross-section values obtained with the precollimated beams as compared to the values found when no precollimation is employed. Furthermore, the intensity and profile of the incident beam are essentially unchanged, showing in addition that the He<sup>+</sup> beam which is incident on the charge-exchange region is a paraxial beam. The consistency between the cross-section values determined in the present experiment and those of other laboratories, where fast He beams are generated under quite different conditions, seems to indicate that metastables do not have a large effect on measurements of this type.

Figure 2 shows a typical detected beam profile. Reproducible total-cross-section data are obtained only when the detector is set at the center of the profile. Beam-profile data are recorded each day and care is taken to operate at the peak of the profile. After the detector is properly positioned, gas is admitted to the scattering chamber and the pressure is first increased to its maximum value and then decreased to "zero." An X-Y recorder

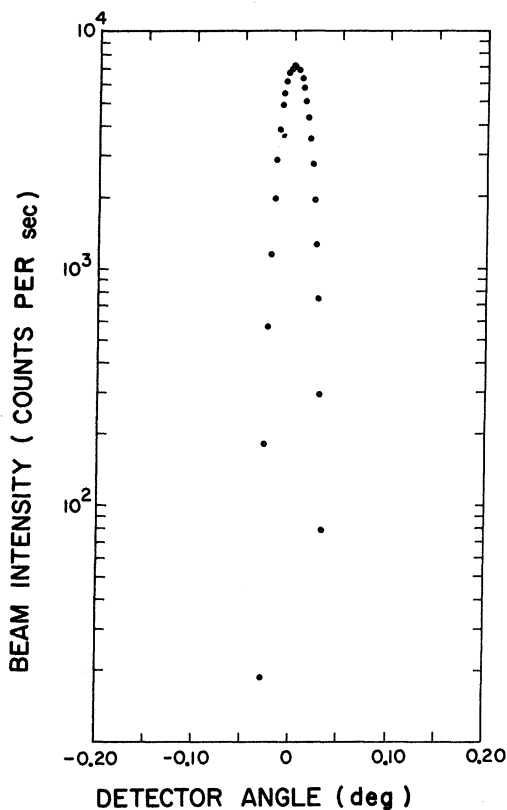


FIG. 2. A typical beam profile taken with a detector angular resolution of  $0.056^\circ$ .

plots the count rate as a function of pressure. Failure to retrace the same curve on increase and decrease of the scattering pressure is sufficient reason to discard the data. This procedure is extremely useful in eliminating errors due to fluctuations in the beam or in the scattering-gas pressure. To check for consistency the starting energy is repeated as the last run each day; in addition, the starting energy is changed from day to day. Cross sections are obtained from the attenuation plots with the aid of Eq. (1) rewritten as

$$\sigma(E) = \frac{3 \cdot 10 \times 10^{-17}}{l_0(1+\alpha)p} \ln\left(\frac{I_0}{I}\right), \quad (2)$$

where  $\sigma(E)$  is in units of  $\text{cm}^2$  when  $l_0$  is in units of cm and  $p$  is in units of Torr. The  $1+\alpha$  term accounts for scattering both in the scattering chamber and along the beam path in the source and detector chambers. In the present experiment  $\alpha$  is approximately 0.001. The beam intensity is found at ten different pressures in each attenuation run. A least-squares fit made by computer determines a single value of  $\sigma(E)$  from the ten sets of intensity and pressure values obtained from the run.

The  $0.056^\circ$  detector-angular-resolution data are taken using an ionization gauge to measure the

scattering pressure. Because of uncertainties in the measured pressure the data are normalized to a cross-section value determined each day at 2.50 keV. The normalizing value at 2.50 keV is determined from a smooth curve drawn through the region of 2.50 keV on a plot of cross section versus energy (from the original data). Absolute cross sections are later determined from the relative data by using a capacitance manometer in a total-cross-section measurement at 2.50 keV. Our later data, at  $0.260^\circ$  detector angular resolution, are taken with a capacitance manometer at all energies and absolute cross sections are directly obtained.

Small-angle differential scattering measurements are also made in a search for structure which may indicate inelastic contributions to the measured total cross sections (the presence of inelastic scattering could cause difficulties in determining a potential from total-cross-section data). For our differential measurements the geometric angular resolutions of the incident beam and detector are changed to  $0.091^\circ$  and  $0.126^\circ$  to increase the scattered signal at the larger angles. Additional small-angle measurements are made to determine the contribution of ionizing collisions to the measured cross sections.

#### IV. EXPERIMENTAL RESULTS

Figure 3 shows the energy dependence of the total cross section obtained in the present experiment as compared to some previously published results of Jordan and Amdur<sup>2</sup> and Belyaev and Leonas.<sup>3</sup> The effect of detector angular resolution on the measured total cross sections is clearly demonstrated in the figure. Curves A and B refer to the present experiment and are the results obtained with geometric angular resolutions of  $0.260^\circ$  and  $0.056^\circ$ , respectively. The resolutions in both the Amdur and Leonas experiments are reported as "effective"<sup>2</sup> resolutions and are  $0.57^\circ$  and  $0.11^\circ$ , respectively. Table I gives the results of our measurements for the two angular resolutions. Errors in the determination of the cross-section values from the experimental data are introduced primarily by a 5% uncertainty in the scattering-gas pressure. Other sources of error are associated with uncertainties in the beam energy and the length of the scattering path, and with the measured beam intensities. The beam energy is generally known to within a few volts; the scattering-cell length is known to an accuracy of better than 1%. The statistical errors in Table I primarily contain contributions from uncertainties in beam intensity and pressure measurements.

Figure 4 shows the differential scattering of He by He at 1.80 and 3.00 keV. This measurement is made by rotating the detector end of the appara-

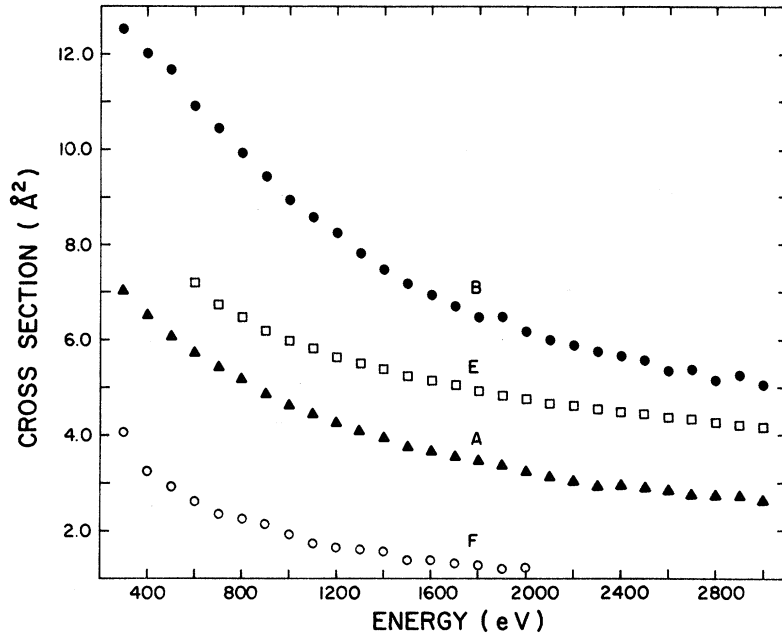


FIG. 3. Comparison of cross-section results (A and B) with reported results of Belyaev and Leonas (E) and Jordan and Amdur (F).

tus about a point in the scattering chamber. The procedure is similar to that employed in the differential measurements of Ref. 8. The results are normalized so that the unscattered beam in-

tensities at each energy are equal. There is no marked structure apparent at either energy. Figure 5 shows the results of a search for ionizing

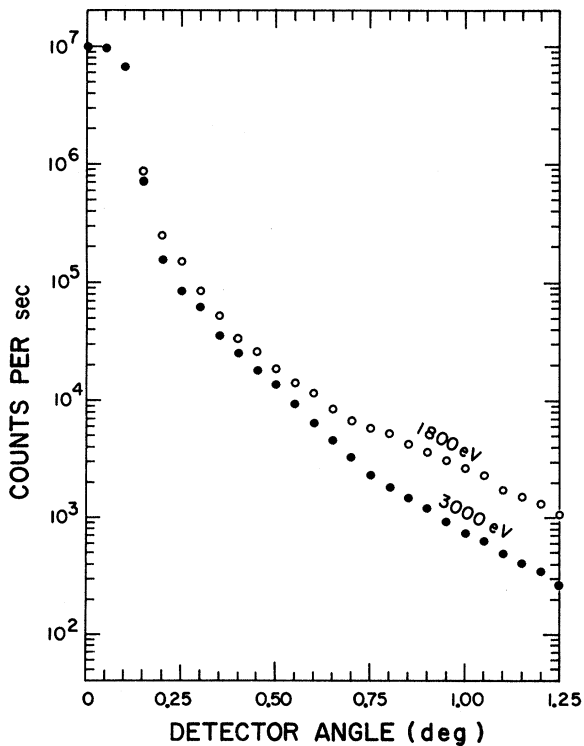


FIG. 4. Scattered signal as a function of angle for He-He collisions at incident energies of 1.80 and 3.00 keV.

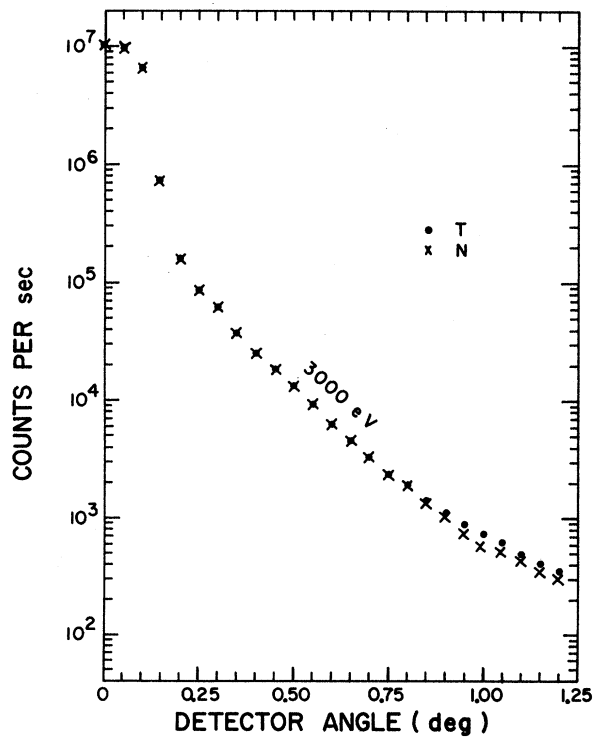


FIG. 5. Scattered signal showing evidence of ionization resulting from the scattering of He by He at 3.00 keV. T refers to the total scattered signal and N refers to the neutral scattered signal.

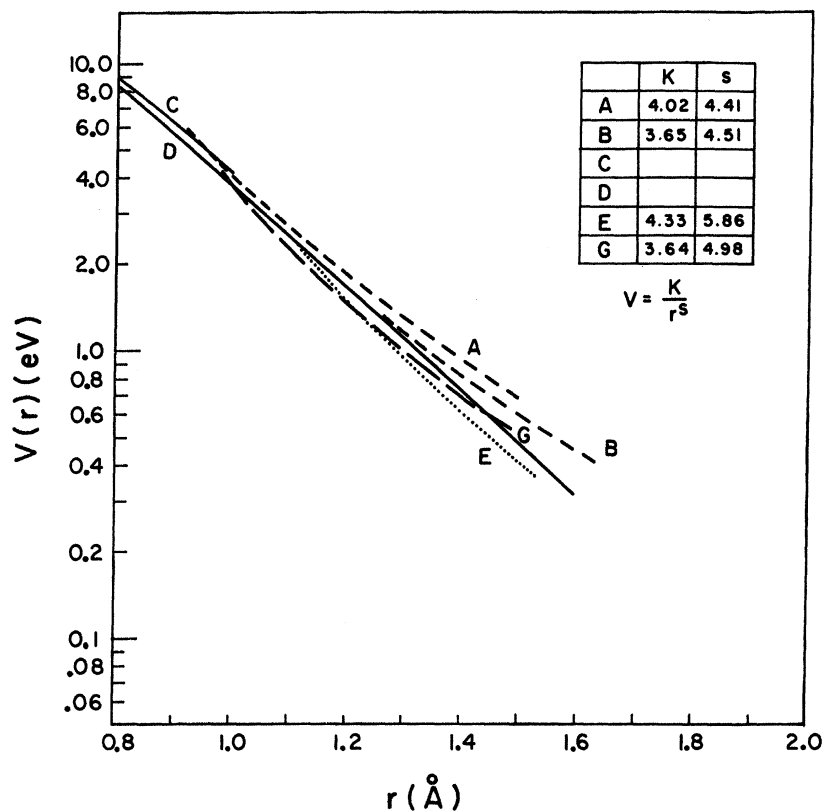


FIG. 6. Comparison of some of the current potential values determined experimentally and theoretically: this experiment (A and B), Belyaev and Leonas (E), Amdur (G), Phillipson (C), and Abrahamson (D).

collisions at 3.00 keV. The curve labeled T represents all particles (regardless of charge state) that reach the detector while N represents neutrals only. Note that curves T and N begin to diverge at an angle of about  $0.80^\circ$  with the T curve lying above the N curve. The difference in value between T and N at each angle is attributed to ions in the scattered beam. At this energy the ratio of ions to totals increases with increasing angle and has a value of approximately 10% at  $1.25^\circ$ . Similar measurements at 1.80 keV show no marked ionization out to a  $1.25^\circ$  scattering angle. In addition, no ionization is observed in the forward-scattered particles at either energy. Since the contribution of ionizing collisions to the measured total cross section is small, even at our highest energy, it appears reasonable to neglect it in determining a potential from total-cross-section data. The usual analysis enabling potentials to be extracted from total-cross-section measurements is based on the assumption that classical scattering theory is applicable. The minimum angle to which a classical analysis is applicable is estimated to be  $0.05^\circ$  at 1 keV ( $0.5^\circ$  at 0.01 keV).<sup>6</sup> One of our angular resolutions is selected to be sufficiently high so that quantum effects could be expected at energies below 1 keV. Curve B of Fig. 3 is taken at this higher resolution and shows that there is no marked de-

TABLE I. Total cross section for the scattering of He by He at detector angular resolutions of  $0.056^\circ$  and  $0.260^\circ$ . S is the standard deviation and  $n$  the number of runs.

Energy (eV)	$0.056^\circ$			$0.260^\circ$		
	Total cross section ( $10^{-16}$ cm <sup>2</sup> )	$S/\sqrt{n}$ ( $10^{-16}$ cm <sup>2</sup> )	$n$	Total cross section ( $10^{-16}$ cm <sup>2</sup> )	$S/\sqrt{n}$ ( $10^{-16}$ cm <sup>2</sup> )	$n$
300	12.51	0.28	54	7.03	0.18	19
400	12.02	0.28	50	6.54	0.18	16
500	11.68	0.36	34	6.11	0.18	14
600	10.91	0.27	46	5.75	0.15	16
700	10.44	0.26	38	5.43	0.17	13
800	9.90	0.22	46	5.18	0.14	16
900	9.40	0.23	39	4.88	0.15	14
1000	8.93	0.17	43	4.63	0.15	16
1100	8.59	0.17	37	4.43	0.17	14
1200	8.24	0.14	45	4.26	0.14	16
1300	7.80	0.17	35	4.06	0.16	14
1400	7.49	0.12	42	3.96	0.15	16
1500	7.19	0.14	36	3.75	0.15	14
1600	6.94	0.09	46	3.69	0.14	15
1700	6.71	0.10	36	3.58	0.16	14
1800	6.49	0.08	48	3.48	0.14	15
1900	6.49	0.10	37	3.38	0.16	14
2000	6.19	0.08	47	3.24	0.13	16
2100	6.10	0.09	39	3.14	0.16	14
2200	5.88	0.05	47	3.07	0.13	17
2300	5.74	0.08	36	2.97	0.15	14
2400	5.66	0.06	47	2.95	0.13	16
2500	5.58	0.05	57	2.91	0.12	16
2600	5.33	0.05	46	2.88	0.12	16
2700	5.37	0.07	30	2.78	0.13	14
2800	5.14	0.05	44	2.78	0.12	16
2900	5.23	0.07	30	2.75	0.11	16
3000	5.03	0.06	55	2.65	0.08	24

parture from the expected behavior, as suggested by the other curves on the figure.

An interatomic potential for the He-He system is calculated using the data in Table I. It is assumed that the general form of the potential is  $V(r) = Kr^{-s}$ . For such a potential  $K$  and  $s$  may be found<sup>10</sup> from

$$\sigma(\theta_0, E) = \pi \left( \frac{c_s K}{E \theta_0} \right)^{2/s} \left( 1 - \frac{(m_1 + m_2) \theta_0}{m_2 c_s} \right), \quad (3)$$

where  $\theta_0$  is the angular resolution,  $E$  is the incident energy, and

$$c_s = \frac{(\pi)^{1/2} \Gamma[\frac{1}{2}(S+1)]}{\Gamma(\frac{1}{2}S)}. \quad (4)$$

With the aid of a computer a least-squares fit of the data is made to the above equation and the results are shown in Fig. 6. Curves B and A are, respectively, the potentials for the 0.056°- and 0.260°-resolution data. Curves C and D are the result of calculations done by Phillipson<sup>11</sup> and Abrahamson.<sup>12</sup> Both (E) and (G) are experimental results; E is that reported by Belyaev and Leonas<sup>3</sup> and G is a result from a review article written by Amdur.<sup>13</sup> The present experiment yields potentials whose values are generally higher than those obtained in the earlier experimental studies. At small internuclear separation there is a reasonably good agreement between our results and the theory, while at the larger internuclear separations our potentials lie above those predicted by theory.

†Supported by the U. S. Army Research Office-Durham, the Connecticut Research Commission, and the University of Connecticut Research Foundation.

\*From part of a thesis submitted by W. J. Savola, Jr. to the Graduate School of the University of Connecticut in partial fulfillment of the requirements for the Ph.D. degree, June, 1971.

<sup>1</sup>I. Amdur, J. E. Jordan, and S. O. Colgate, *J. Chem. Phys.* **34**, 1525 (1961).

<sup>2</sup>J. E. Jordan and I. Amdur, *J. Chem. Phys.* **46**, 165 (1967).

<sup>3</sup>Y. N. Belyaev and V. B. Leonas, *Dokl. Akad. Nauk SSSR* **173**, 306 (1967) [*Sov. Phys. Dokl.* **12**, 233 (1967)].

<sup>4</sup>A. B. Kannev and V. B. Leonas, *Dokl. Akad. Nauk SSSR* **162**, 798 (1965) [*Sov. Phys. Dokl.* **10**, 529 (1965)].

<sup>5</sup>Y. N. Belyaev and V. B. Leonas, *Dokl. Akad. Nauk SSSR* **170**, 1039 (1966) [*Sov. Phys. Dokl.* **11**, 866 (1967)].

<sup>6</sup>E. A. Mason and J. T. Vanderslice, in *Atomic and Molecular Processes*, edited by D. R. Bates (Academic, New York, 1962), Chap. 17.

<sup>7</sup>S. W. Nagy, W. J. Savola, Jr., and E. Pollack, *Phys. Rev.* **177**, 71 (1969).

<sup>8</sup>S. W. Nagy, S. M. Fernandez, and E. Pollack, *Phys. Rev. A* **3**, 280 (1971).

<sup>9</sup>D. C. Lorents, W. Aberth, and V. W. Hesterman, *Phys. Rev. Lett.* **17**, 849 (1966).

<sup>10</sup>E. H. Kennard, *Kinetic Theory of Gases* (McGraw-Hill, New York, 1938), Chap. 3.

<sup>11</sup>P. E. Phillipson, *Phys. Rev.* **125**, 1931 (1962).

<sup>12</sup>A. A. Abrahamson, *Phys. Rev.* **130**, 693 (1963).

<sup>13</sup>I. Amdur, in *Atomic Interactions [A]*, edited by B. Bederson and W. L. Fite (Academic, New York, 1962), Chap. 3.2.

## Scattering between Hg Atoms and Light Atomic Projectiles of keV Energies\*

A. van Wijngaarden and W. E. Baylis

*Department of Physics, University of Windsor, Windsor, Ontario, Canada*

(Received 28 September 1972)

Previously described measurements for the scattering of  $^1\text{H}^+$ ,  $^4\text{He}^+$ ,  $^{11}\text{B}^+$ , and  $^{14}\text{N}^+$  ions of energies  $9 < E < 75$  keV by a thermal beam of Hg atoms have been extended to smaller angles. Angular distributions for  $2.8 < \theta_L < 40$  deg have been measured for the scattering of all projectiles independent of final charge state. Differential scattering cross sections are in approximate agreement with the theory for scattering in a Thomas-Fermi potential over a range of five orders of magnitude. When the cross sections are reduced by the Lindhard procedure, we find that the Thomas-Fermi interaction is a better approximation to the actual potential than the Lenz-Jensen interaction.

### I. INTRODUCTION

In a recent publication<sup>1</sup> we presented data for elastic scattering of keV projectiles from Hg atoms. Measured differential-scattering cross sections

for large deflection angles ( $\theta_L > 15^\circ$ ) were found to be in fairly good agreement with theory for the Thomas-Fermi (TF) model of the atom. The present work describes the extension of these experiments to smaller scattering angles ( $\theta_L \geq 2.8^\circ$ ) with